Author Manuscript

Author Manuscript

Author Manuscript

Author Manuscript

HHS Public Access

Author manuscript

Cardiovasc Pathol. Author manuscript; available in PMC 2018 December 17.

Published in final edited form as:

Cardiovasc Pathol. 2014 ; 23(6): 335–343. doi:10.1016/j.carpath.2014.06.003.

Human cardiac fibroblast extracellular matrix remodeling: dual effects of tissue inhibitor of metalloproteinase-2

Janet M.C. Ngu[a], **Guoqi Teng**[a], **Hans Christopher Meijndert**[a], **Holly E. Mewhort**[a], **Jeannine D. Turnbull**[a], **William G. Stetler-Stevenson**[b], and **Paul W.M. Fedak**[a,*]

[a]Section of Cardiac Surgery, Department of Cardiac Sciences, University of Calgary, Libin Cardiovascular Institute of Alberta, Calgary, Alberta, Canada

[b]Center for Cancer Research, National Cancer Institute, Bethesda, MD, USA

Abstract

Objective: Tissue inhibitor of metalloproteinase-2 (TIMP-2) is an endogenous inhibitor of matrix metalloproteinases (MMPs) that attenuates maladaptive cardiac remodeling in ischemic heart failure. We examined the effects of TIMP-2 on human cardiac fibroblast activation and extracellular matrix (ECM) remodeling.

Methods: Human cardiac fibroblasts within a three-dimensional collagen matrix were assessed for phenotype conversion, ECM architecture and key molecular regulators of ECM remodeling after differential exposure to TIMP-2 and Ala+TIMP-2 (a modified TIMP-2 analogue devoid of MMP inhibitory activity).

Results: TIMP-2 induced opposite effects on human cardiac fibroblast activation and ECM remodeling depending on concentration. TIMP-2 activated fibroblasts into contractile myofibroblasts that remodeled ECM. At higher concentrations (N10 nM), TIMP-2 inhibited fibroblast activation and prevented ECM remodeling. As compared to profibrotic cytokine transforming growth factor (TGF)-beta1, TIMP-2 activated fibroblasts and remodeled ECM without a net accumulation of matrix elements. TIMP-2 increased total protease activity as compared to TGF-beta1. Ala+TIMP-2 exposure revealed that the actions of TIMP-2 on cardiac fibroblast activation are independent of its effects on MMP inhibition. In the presence of GM6001, a broad-spectrum MMP inhibitor, TIMP-2-mediated ECM contraction was completely abolished, indicating that TIMP-2-mediated fibroblast activation is MMP dependent.

Conclusion: TIMP-2 functions in a contextual fashion such that the effect on cardiac fibroblasts depends on the tissue microenvironment. These observations highlight potential clinical challenges in using TIMP-2 as a therapeutic strategy to attenuate postinjury cardiac remodeling.

Keywords

TIMP-2; Extracellular matrix; Cardiac fibroblasts; Remodelling; Human cells

[*]Corresponding author. C880, 1403-29 Street NW, Calgary, Alberta, Canada T2N 2T9. Tel.: +1 403 944-5931; fax: +1 403 270 3715., paul.fedak@gmail.com (P.W.M. Fedak).

Author Manuscript Author Manuscript Author Manuscript Author Manuscript

1. Introduction

Tissue inhibitor of metalloproteinase-2 (TIMP-2) is a critical regulator of tissue remodeling. TIMP-2 is constitutively expressed in most cell types [1] and has diverse actions within the extracellular matrix (ECM) microenvironment. TIMP-2 inhibits a broad spectrum of matrix metalloproteinases (MMPs) [2] and retains some biologic actions that are independent of its MMP-inhibitory activity [3,4]. The actions of TIMP-2 are complex and sometimes paradoxical. For example, TIMP-2 inhibits MMP-2 activity, but also facilitates cell surface activation of pro-MMP-2 by selective interaction with membrane type 1-MMP (MT1-MMP), forming a tri-molecular complex of TIMP-2/Pro-MMP-2/MT1-MMP [5]. MMP-2 plays a critical role in maladaptive ECM remodeling after cardiovascular injury. Given that TIMP-2 can both suppress and stimulate MMP-2 activity, and in light of its MMP-independent bioactivity, the role of TIMP-2 on cardiovascular cells and tissue remodeling is poorly understood.

Cardiac fibroblasts regulate ECM homeostasis through synthesis of ECM components and secretion of MMPs and TIMPs [6]. After myocardial infarction (MI), fibroblasts become activated to myofibroblasts. Ongoing and persistent myofibroblast activity disrupts ECM homeostasis and causes maladaptive post-MI cardiac remodeling. Myocardial TIMP-2 levels are reduced during the late phase of post-MI ventricular remodeling [7]. In a rodent MI model, TIMP-2 deletion worsened infarct expansion and ventricular dilatation [8], whereas myocardial TIMP-2 overexpression at the time of MI significantly improved survival and limited maladaptive cardiac remodeling [9]. We previously determined that vascular smooth muscle cell transplantation induced TIMP-2 expression and limited post-MI maladaptive remodeling [10]. These data and others suggest that TIMP-2, through its effects on ECM homeostasis, may be an important therapeutic target for antiremodeling strategies after cardiac injury. Paradoxically, Lovelock and colleagues [11] observed that TIMP-2 induced a profibrotic response in cultured murine cardiac fibroblasts. As compared to other TIMP species, TIMP-2 uniquely activated myofibroblasts and increased collagen synthesis. Before clinical translation of TIMP-2 therapeutically, the effects of TIMP-2 on cardiac fibroblasts and ECM remodeling should be determined.

We examined the effects of TIMP-2 on human cardiac fibroblast-mediated ECM remodeling within three-dimensional (3D) collagen matrices. We explored the MMP-independent actions of TIMP-2 using a modified analogue of TIMP-2 (Ala+) devoid of MMP-inhibitory activity while maintaining its tertiary protein structure [12]. This is the first study to outline the effects of TIMP-2 on fibroblast regulation and ECM remodeling in human cardiac cells.

2. Materials and methods

2.1. Human cardiac fibroblast isolation and expansion

Right atrial appendage biopsies (N=6) were obtained from consenting patients undergoing routine cardiac surgery at Foothills Medical Center (Calgary, Alberta). Patients underwent coronary artery bypass grafting or valve replacement surgery. No patients had extensive structural atrial remodeling. All experiments involving human tissue were approved by Conjoint Health Research Ethics Board at the University of Calgary and conform to the

Author Manuscript Author Manuscript Author Manuscript Author Manuscript

Declaration of Helsinki. Samples were minced and dissociated in 0.2% Collagenase Type II at 37°C in an Isotemp Dry Bath (Fisher Scientific) with gentle shaking. Cell suspension was collected and remnant tissue was removed using tissue strainer of 40 μm pore size (BD Falcon). Collected cells were centrifuged at 1500 RPM (rotations per minute) for 5 min at room temperature (RT). Cell pellet was subsequently seeded in complete medium composed of Iscove's modified Dulbecco's medium (IMDM) supplemented with 10% fetal bovine serum plus 50,000 units of penicillin and 50,000 mg of streptomycin. Cells were cultured in an incubator at 37°C with a 5% CO_2 atmosphere. Cells from passages 4 to 8 were used.

2.2. Characterization of human cardiac fibroblasts

Immunohistochemistry staining was used to characterize the cultured cells. Cells were seeded on coverslips prior to fixation with 4% paraformaldehyde (PFA) at RT for 20 min, then simultaneously blocked and permeabilized at RT for 1 h by incubation in blocking buffer (2% goat serum and 1% bovine serum albumin in 1× PBS) containing 0.1% Triton X-100. Next, coverslips were incubated in corresponding primary antibody, all at 1:500 dilution unless otherwise stated: mouse anti-fibronectin (Calbiochem), mouse anti-fibroblast surface protein (Sigma-Aldrich), rabbit anti-smooth muscle-22-a (1:200 dilution; Abcam), rabbit anti-vimentin, rabbit anti-discoidin domain receptor 2, rabbit anti-troponin I, rabbit anti-desmin or rabbit anti-von Willibrand Factor (Santa Cruz Biotechnology) at 4°C overnight with gentle shaking. After washing in blocking buffer, coverslips were then incubated in secondary antibody at 1:500 dilution, either Alexa Fluor 633 goat anti-mouse or Alexa Fluor 633 goat anti-rabbit, for 1 h at RT with gentle shaking. Lastly, coverslips were washed with blocking buffer and then mounted onto microscope glass slide in Prolong Gold Antifade Reagent (Invitrogen) containing DAPI for counterstaining of nuclear visualization. All fluorescent images were captured using confocal laser microscopy (LSM 5, Carl Zeiss Microscopy, Thornwood, NY, USA) and processed using Zen software (Carl Zeiss Microscopy).

2.3. Assessment of 3D collagen ECM remodeling

Cultured human cardiac fibroblasts were serum starved for 24 h. Cells were trypsinized and added to a liquid form of neutralized rat-tail type I collagen (BD Biosciences) at a final concentration of 1.8 mg/ml. The liquid gel mixture containing cells was kept on ice during the preparation. On a 24-well-plate, 400 μl of the liquid gel mixture containing 2.5×10^5 cells/ml was dispensed into each well and incubated at 37°C for at least 1 h to allow for gel polymerization. Immediately after polymerization, 500 μl of IMDM either alone [serum-free medium (SFM)] or containing 10 ng/ml human recombinant transforming growth factor (TGF)-beta1 (Gibco-Invitrogen, Frederick, MD, USA), 10 nM human recombinant TIMP-2 (Calbiochem, EMD Biosciences Inc., La Jolla, CA, USA), 10 nM Ala+TIMP-2 (gift from Dr. Stetler-Stevenson, NIH), 10 nM human recombinant TIMP-3 (R&D Systems Inc, Minneapolis, MN, USA), TIMP-2 (10 nM)+50 nM GM6001 (Calbiochem, EMD Biosciences Inc.) or 100 ng/ml human recombinant MMP-2 (R&D Systems Inc) was added to each well. MMP-2 was activated by incubating in 0.05 M borate (pH 9.0), 0.01 mM $ZnCl_2$, 5 mM $CaCl_2$ and 0.5 mM APMA (aminophenylmecuric acetate; Sigma) at 37°C for 30 min. Plates were further incubated overnight in a 37°C incubator with a 5% CO_2 atmosphere. To initiate ECM contraction, the cell–ECM constructs were released from the

Author Manuscript Author Manuscript Author Manuscript Author Manuscript

well wall using a sterile microspatula (Corning). Serial images of the ECM dimensions were obtained from the time of release (baseline) and at 24 h. Image J analysis software (NIH, USA) was used to measure the area of ECM contraction as a quantitative measure of ECM remodeling.

2.4. Cell number and viability

Cells were released from collagen ECM by incubating the constructs in 100 μl of 500 units/ml collagenase type II in 37°C water bath with constant agitation until the ECM was completely dissolved. Subsequently, the cell suspension was centrifuged at 1500 RPM for 5 min. Cell pellet was resuspended in 1 ml of IMDM and 0.1 ml of 0.4% trypan blue stain (GIBCO). Ten microliters of cell suspension was loaded onto a hemacytometer, and then the total cell number and the number of blue-stained cells were counted. Cell viability (%) was calculated using the formula as below:

$$\text{Cell viability (\%)} = [1.0 - (\text{number of blue cells/number of total cells})] \times 100$$

2.5. Confocal laser scanning microscopic analysis

Constructs were fixed in 4% PFA at RT for 30 min and simultaneously blocked and permeabilized at RT for 1 h by incubating in blocking buffer containing 0.1% Triton X-100. Constructs were incubated in primary antibody (mouse anti-a-SMA at 1:500; Sigma-Aldrich) at 4°C for 48 h with gentle shaking, followed by washing and incubated in secondary antibody (Alexa Fluor 488 goat anti-mouse at 1:500; Invitrogen) at RT for 1 h with gentle shaking. Lastly, constructs were briefly washed then mounted onto microscope glass slides in Prolong Gold Antifade Reagent containing DAPI for nuclear visualization. All fluorescent images were captured using confocal laser microscopy (LSM 5; Carl Zeiss) in Z-stack module and processed using Zen software. To enable comparison between images, all microscopic settings were set identically for each image under all experimental conditions. The proportion of construct volume that was positive for alpha-SMA expression was quantified. Z-stack images were taken from eight random fields. The acquired stack of images from each random field was used to reconstruct a 3D image using Volocity software (PerkinElmer) that consists of a definite volume, defined as “total image volume.” The image volume-stained positive for a-SMA was measured and was defined as “alpha-SMA-positive image volume.” The alpha-SMA expression of the cells embedded in each cell-ECM construct was calculated using the formula below:

$$\text{proportion of } \alpha\text{-SMA-positive volume} = \frac{\alpha\text{-SMA-positive image volume}}{\text{Total image volume}} \times 100\%$$

2.6. Extracellular matrix architecture

To visualize the content and spatial architecture of collagen in the matrices, confocal reflection microscopy (CRM) was performed using a confocal laser microscopy (LSM 5; Carl Zeiss). CRM collects auto-fluorescent signals reflected by the matrix fibers and allows for 3D structural reconstruction of the matrix [13]. Constructs were excited with a low-

Author Manuscript Author Manuscript Author Manuscript Author Manuscript

density 405 nm laser and the emitted light between 420 and 480 nm was collected. Z-stack images of each construct were acquired and reconstructed using Volocity software (PerkinElmer) to facilitate a qualitative assessment of the collagen fibril network (content and spatial organization) within each construct.

2.7. In situ zymography

In situ zymography was modified for application with functional collagen gel contraction assay as described by previous studies [14,15]. In brief, constructs containing human cardiac fibroblasts were prepared as described in the previous section. DQ Gelatin-FITC (Molecular Probes) emits green fluorescent signals when cleaved by proteases that can be quantified. DQ Gelatin-FITC was added to the liquid gel solution at a final concentration of 10 μg/ml prior to gel polymerization, followed by targeted treatments. Subsequently, constructs were fixed in 4% PFA for 30 min at RT and washed with PBS before mounted on microscope glass slide with Prolong Gold Antifade Reagent. Z-stack images from eight random fields of each collagen gel were captured using confocal laser microscopy (LSM 5; Carl Zeiss), and images were analyzed using Volocity software (PerkinElmer). Bright green fluorescent spots indicating proteolytic digestion in the acquired 3D gel image were identified as “green fluorescent objects” on the Volocity software platform, and the total volume of these objects was summed as “total volume of green fluorescence.” Mean fluorescence intensity of each analyzed 3D gel image was generated automatically by the Volocity software, by averaging the fluorescence intensity of all the “green fluorescent objects” identified in the image. The total green fluorescence activity, known to be proportionate to the total protease activity, was calculated by multiplying the total volume of green fluorescence of each 3D image by its mean fluorescence intensity. The total protease activity in collagen gel normalized to the corresponding 3D gel image volume to allow for comparison between images:

$$\text{Total protease activity} = \frac{\text{mean fluorescence intensity} \times \text{total volume of green fluorescence}}{\text{total image volume}}$$

2.8. Collagen synthesis

To estimate collagen synthesis, cell–ECM constructs were immunostained with mouse anti-pro-collagen I (1:200 dilution; Developmental Studies Hybridoma Bank) and subsequently developed with Alexa Fluor 633 goat anti-mouse (1:500 dilution; Invitrogen). Constructs were mounted in Prolong Gold Antifade Reagent (Molecular Probes) containing DAPI. 3D images were reconstructed using Volocity software (PerkinElmer) as previously described. Cells positive for pro-collagen I were counted and divided by the total DAPI (nuclei) for each image. Pro-collagen I-positive cells of eight random images from each group were averaged and expressed as a percentage (%) of the total cell number.

2.9. Statistical analysis

All group data are presented as mean±S.D. Data were obtained from a representative experiment of which each was repeated in triplicate. When only two groups were compared, Student’s *t* test was performed. For comparison of more than two groups, one-way analysis of variance was used and followed by appropriate post hoc comparison tests. All statistical

Author Manuscript Author Manuscript Author Manuscript Author Manuscript

analyses were performed using GraphPad Prism 6.0, with $P<.05$ considered statistically significant.

3. Results

3.1. Confirmation of human cardiac fibroblast phenotype

The morphology of the cultured cells was examined using phase-contrast light microscopy and was consistent with fibroblasts (Fig. 1A). To further characterize the cells, immunocytochemistry was performed to confirm the presence of several fibroblast-specific markers: fibronectin, vimentin, fibroblast surface protein and discoidin domain receptor-2. Greater than 95% of the cultured cells from passage 4 stained positive for fibroblast markers (Fig. 2). Several nonfibroblast markers were used to rule out other cell types found in the heart (Fig. 2). Specifically, cells were negative for SM22-alpha (smooth muscle cells), troponin-I (cardiomyocytes), desmin (smooth muscle cells, skeletal muscle cells, cardiomyocytes) and von Will-ebrand factor (endothelial cells).

3.2. Concentration-dependent effects of TIMP-2 on ECM remodeling

Embedded cardiac fibroblasts contract collagen matrices in proportion to the extent of their differentiation into myofibroblasts [16,17]. TGF-beta1 stimulates cardiac fibroblasts to undergo phenotypic conversion into myofibroblasts and induce ECM remodeling as determined by the extent of contraction [17]. We examined the differential effects of increasing concentrations of TIMP-2 on collagen ECM remodeling (Fig. 3A). TIMP-2 exerted opposing effects on ECM contraction at different concentrations. Lower concentrations of TIMP-2 stimulated ECM contraction, whereas higher concentrations inhibited ECM contraction. We observed the highest degree of ECM contraction from TIMP-2 at a concentration of 10 nM. We further examined the effects of TIMP-2 on collagen ECM remodeling at this concentration. We compared the differential effects of 10 nM TIMP-2 with exogenous TGF-beta1 (10 ng/ml), 10 nM Ala+TIMP-2 (devoid of MMP inhibitory activity) and 10 nM TIMP-3 on collagen ECM remodeling (Fig. 3B and C). Both exogenous TGF-beta1 and TIMP-2 stimulated ECM contraction. Ala+TIMP-2 yielded a similar magnitude of ECM contraction as TIMP-2, indicating that the stimulatory effect of TIMP-2 is independent of its MMP-inhibitory actions. Interestingly, induction of ECM remodeling was not observed with a matched concentration of TIMP-3, suggesting that TIMP-induced fibroblast activation is specific and unique to TIMP-2.

3.3. TIMP-2 induces phenotypic differentiation of human cardiac fibroblasts

Differentiated myofibroblasts are defined by the presence of a-SMA and up-regulated collagen synthesis [18]. We observed that all groups with increased ECM contraction (TGF-beta1, 10 nM TIMP-2 and 10 nM Ala+TIMP-2) exhibited a higher expression of alpha-SMA (Fig. 4A andB). Both TIMP-2 and Ala+TIMP-2 stimulated the morphological transformation toward myofibroblast-like features (Fig. 4A). Treatment with TGF-beta1 and TIMP-2 did not significantly alter the cell number and cell viability of the cells within collagen ECM (Fig. 4C). Collectively, these data confirm that TIMP-2 and Ala+TIMP-2 induce collagen ECM remodeling, at least in part, by stimulating phenotypic conversion of cardiac fibroblasts into myofibroblasts.

Author Manuscript Author Manuscript Author Manuscript Author Manuscript

3.4. TIMP-2 does not induce ECM deposition

By confocal microscopy, 3D images of collagen ECM architecture were reconstructed to visualize collagen fibril network content and organization (Fig. 5). TGF-beta1 increased collagen fibril density demonstrating a net fibrotic response (Fig. 5: second row). Paradoxically, we did not observe the same fibrotic response in both the TIMP-2 and the Ala+TIMP-2 groups (Fig. 5: third row & fourth row). In addition, TIMP-3 did not significantly alter the collagen ECM architecture as compared to the SFM group (Fig. 5: bottom row). Collagen ECM remodeling was independent of the alteration in the collagen fibril organization and content. This observation is in agreement with current literature [19].

3.5. TIMP-2 increases total protease activity

In situ zymography and quantitative image analysis was employed to directly measure and compare protease activity in the collagen ECM microenvironment (Fig. 6A and B). TGF-beta1 (10 ng/ml) increased total protease activity. Both TIMP-2 and Ala+TIMP-2 increased protease activity, greater than TGF-beta1. Ala+TIMP-2 induced the greatest increase in protease activity, likely due to its abolished capacity for MMP inhibition. Interestingly, TIMP-3 did not alter total protease activity, further supporting a unique role for TIMP-2 in regulating ECM homeostasis. At a low concentration, TIMP-2 induced a net increase in total protease activity within ECM.

3.6. TIMP-2 induces collagen synthesis

TGF-beta1 induced a significant increase in human cardiac fibroblast pro-collagen I expression as compared to SFM (89.7%±5.8% vs. 81.8%±5.6%, $P<.05$). TIMP-2 induced pro-collagen I expression similar to TGF-beta1 (91.9%±5.5%, P=NS) and significantly increased as compared to SFM ($P<.01$). Devoid of MMP-inhibitory actions, Ala+TIMP-2 induced pro-collagen I expression in cardiac fibroblasts) as compared to SFM (87.4±4.2%, $P<.05$) with a level similar to TGF-beta1 and TIMP-2. This observation indicates that TIMP-2 induction of collagen synthesis is independent of its MMP inhibition.

3.7. TIMP-2 induces collagen ECM remodeling by MMP activation

Increased MMP abundance and activity is associated with increased collagen ECM remodeling [20,21]. In support, we observed that activated MMP-2 increased human cardiac fibroblast-mediated ECM remodeling (Fig. 7A and B). An exogenous MMP inhibitor, GM6001 (50 nM), completely abolished TIMP-2-induced ECM contraction (Fig. 7C and D). These observations collectively suggest that TIMP-2 induces collagen ECM remodeling by increasing MMP activity, a known effect of TIMP-2 at lower concentrations [5].

4. Discussion

In animal models of human disease, TIMP-2 is reported to exert beneficial effects in attenuating adverse post-MI cardiac remodeling [8–10]. TIMP-2 is a complex protein with paradoxical effects on MMP activities. Lovelock and colleagues [11] examined the differential effects of various TIMP species in modulating murine cardiac fibroblasts. As compared to all other TIMP species, TIMP-2 was observed to induce the most profound increase in murine myofibroblast activation and collagen synthesis, suggesting that TIMP-2

Author Manuscript Author Manuscript Author Manuscript Author Manuscript

is profibrotic [11]. Our data highlight a more complex influence of TIMP-2 on human cardiac fibroblasts within an ECM microenvironment. TIMP-2 was found to induce dual and opposite effects depending on concentration.

Our study differs from the work of previous investigators in that we examined human cardiac fibroblasts (as compared to murine or immortalized cell lines) within a 3D collagen matrix (as compared to 2D culture conditions). We believe that this model best mimics the human cardiac ECM microenvironment. Numerous studies show that cultured fibroblasts in a 2D system spontaneously undergo a phenotypic switch to myofibroblasts [22,23]. By using an innovative 3D collagen ECM culture system, we were able to maintain cardiac fibroblasts in a form similar to in vivo resting cells [24]. In addition, given that TIMP-2 concentration can determine its influence on MMP-2 activity, we examined the effects of TIMP-2 over different concentrations. Basal myocardial levels of TIMP-2 are not well documented, but median plasma TIMP-2 levels in humans is estimated to be 163 ng/ml (7.4 nM) in EDTA plasma and 139 ng/ml(6.3 nM) in citrate plasma [25]. We utilized exogenous TIMP-2 in a physiologic range for our experiments.

It is well known that inhibition of MMP activity reduces collagen ECM remodeling and alpha-SMA expression [26]. Intriguingly, our data show that TIMP-2 exerts opposing effects on collagen ECM remodeling at different concentrations, indicating the existence of complex interactions. At low concentrations, TIMP-2 stimulates collagen ECM remodeling, whereas ECM contraction was inhibited at high concentrations. In this study, we focused our efforts on the myofibroblast-activating aspect of TIMP-2 as this effect is deemed to be specific to TIMP-2 as compared to the other TIMP species. Furthermore, we aimed to investigate the mechanisms underlying this compelling phenomenon, in order to expand on the observations of Lovelock and colleagues [11].

A dynamic balance of MMP activity and new collagen synthesis is critical to maintaining ECM homeostasis [27]. Dysregulation of ECM, either with excessive degradation of matrix components or by increased matrix deposition, is implicated in the progression of heart failure [28]. TIMP-2-dependent activation of pro-MMP-2 is a critical and essential regulator of MMP-2 activation [5,8]. In the specific conditions of our study, we observed that TIMP-2 increases total ECM protease activity, much higher than the profibrotic mediator TGF-beta1. We also observed that collagen synthesis was increased by both TGF-beta1 and TIMP-2, but there was no significant difference between these groups. These results may explain our observation that TIMP-2 does not prompt a concomitant net fibrotic response of collagen within the cell–matrix constructs, as does TGF-beta1. Proteolytic activity exceeded new collagen synthesis resulting in preserved ECM architecture despite significant ECM remodeling. Importantly, these data suggest that TIMP-2 can stimulate the activation of fibroblasts at lower concentrations, but it is not profibrotic such that net collagen ECM components are not increased and ECM integrity is preserved.

Several MMPs possess the ability to cleave latent TGF-beta1 and increase its activity [29,30]. In contrast, synthetic MMP inhibitors suppress collagen ECM remodeling [26]. Our data demonstrate that active MMP-2 is capable of inducing human cardiac fibroblast-mediated ECM remodeling. The suppression of TIMP-2-induced ECM contraction by a

Author Manuscript Author Manuscript Author Manuscript Author Manuscript

synthetic MMP inhibitor GM6001 suggests that TIMP-2 induces ECM remodeling by MMP activation. Various actions of TIMP-2 that are independent of its MMP-inhibitory activity have been defined. Ala+TIMP-2 contains a single alanine residue appended to the amino-terminal cysteine of the wild-type TIMP-2 and completely disrupts its MMP inhibitory activity [12]. Several studies have utilized this unique analogue to delineate the actions of TIMP-2 that are independent of MMP inhibition [3,4,31]. We determined that TIMP-2 stimulates cardiac myofibroblast differentiation through mechanisms that are independent of its MMP inhibitory activity given that Ala+TIMP-2 exhibits the same effects as endogenous TIMP-2 on fibroblast-mediated collagen ECM remodeling.

The concept that TIMPs exhibit their beneficial effects on cardiac remodeling solely via their MMP inhibitory actions may be premature, as TIMPs exert diverse biological actions on multiple cell types, which synthetic MMP inhibitors lack. Efforts to use synthetic MMP inhibitors to limit MMP-mediated cardiac remodeling have uniformly failed after clinical translation due to unanticipated adverse effects [32] and limited efficacy [33] in human subjects. Our data support and highlight the complexity of TIMP actions on human cardiac fibro-blasts. Prior data using rodent cells may not be clinically relevant as rodent cardiac basal metabolism varies substantially across different species [34]. Our human cell model would benefit from further validation by comparing clinical characteristics and the baseline state of the atrial tissue with respect to fibrosis and remodeling as the patient's clinical condition may influence cellular activity in the model. It is possible that ventricular fibroblasts may respond differently to TIMP-2. Further studies would be required to confirm a similar response as observed with atrial cells.

To our knowledge, this is the first study to investigate the role of TIMP-2 in regulating human cardiac fibroblasts. While the therapeutic potential of TIMP-2 is recognized, the dual effects of TIMP-2 and narrow therapeutic range suggest that further study may be needed before clinical application of TIMP-2 as a potential antiremodeling agent.

Acknowledgments

Funding: This work was supported by the Heart and Stroke Foundation of Alberta, NWT, and Nunavut. P.W.M.F. is a clinical investigator for Alberta Innovates–Health Solutions (AIHS). H.E.M. receives salary support from the AIHS. W.G.S.-S. was funded by the NCI Center for Cancer Research Intramural Research Program Grant (ZIA-SC009179–22). The authors have no conflicts of interest to disclose.

References

[1]. Nuttall RK, Sampieri CL, Pennington CJ, Gill SE, Schultz GA, Edwards DR. Expression analysis of the entire MMP and TIMP gene families during mouse tissue development. FEBS Lett 2004;563:129–34. [PubMed: 15063736]

[2]. Gomez DE, Alonso DF, Yoshiji H, Thorgeirsson UP. Tissue inhibitors of metalloproteinases: structure, regulation and biological functions. Eur J Cell Biol 1997;74:111–22. [PubMed: 9352216]

[3]. Lee SJ, Tsang PS, Diaz TM, Wei BY, Stetler-Stevenson WG. TIMP-2 modulates VEGFR-2 phosphorylation and enhances phosphodiesterase activity in endothelial cells. Lab Invest 2010;90:374–82. [PubMed: 20084057]

[4]. Seo D, Kim S, Eom S, Yoon H. TIMP-2 disrupts FGF-2-induced downstream signaling pathways. Microvasc Res 2008;76:145–51. [PubMed: 18721821]

Author Manuscript Author Manuscript Author Manuscript Author Manuscript

[5]. Wang Z, Juttermann R, Soloway PD. TIMP-2 is required for efficient activation of proMMP-2 in vivo. J Biol Chem 2000;275:26411–5. [PubMed: 10827175]

[6]. Souders CA, Bowers SL, Baudino TA. Cardiac fibroblast: the renaissance cell. Circ Res 2009;105:1164–76. [PubMed: 19959782]

[7]. Wilson EM, Moainie SL, Baskin JM, Lowry AS, Deschamps AM, Mukherjee R, Guy TS, St John-Sutton MG, Gorman JH, Edmunds LH, Gorman RC, Spinale FG. Region- and type-specific induction of matrix metalloproteinases in post-myocardial infarction remodeling. Circulation 2003;107:2857–63. [PubMed: 12771000]

[8]. Kandalam V, Basu R, Abraham T, Wang X, Soloway PD, Jaworski DM, Oudit GY, Kassiri Z. TIMP2 deficiency accelerates adverse post-myocardial infarction remodeling because of enhanced MT1-MMP activity despite lack of MMP2 activation. Circ Res 2010;106:796–808. [PubMed: 20056917]

[9]. Ramani R, Nilles K, Gibson G, Burkhead B, Mathier M, McNamara D, McTiernan CF. Tissue inhibitor of metalloproteinase-2 gene delivery ameliorates postinfarction cardiac remodeling. Clin Transl Sci 2011;4:24–31. [PubMed: 21348952]

[10]. Fedak PWM, Bai L, Turnbull J, Ngu J, Narine K, Duff HJ. Cell therapy limits myofibroblast differentiation and structural cardiac remodeling: basic fibroblast growth factor-mediated paracrine mechanism. Circ Heart Fail 2012;5:349–56. [PubMed: 22508775]

[11]. Lovelock JD, Baker AH, Gao F, Dong JF, Bergeron AL, McPheat W, Sivasubramanian N, Mann DL. Heterogeneous effects of tissue inhibitors of matrix metalloproteinases on cardiac fibroblasts. Am J Physiol Heart Circ Physiol 2005;288:H461–8. [PubMed: 15650153]

[12]. Wingfield PT, Sax JK, Stahl SJ, Kaufman J, Palmer I, Chung V, Corcoran ML, Kleiner DE, Stetler-Stevenson WG. Biophysical and functional characterization of full-length, recombinant human tissue inhibitor of metalloproteinases-2 (TIMP-2) produced in Escherichia coli. J Biol Chem 1999;274:21362–8. [PubMed: 10409697]

[13]. Harjanto D, Maffei JS, Zaman MH. Quantitative analysis of the effect of cancer invasiveness and collagen concentration on 3D matrix remodeling. PLoS One 2011;6:e24891. [PubMed: 21980363]

[14]. Chhabra A, Jaiswal A, Malhotra U, Kohli S, Rani V. Cell in situ zymography: an in vitro cytotechnology for localization of enzyme activity in cell culture. In Vitro Cell Dev Biol Anim 2012;48:463–6. [PubMed: 22821629]

[15]. Cha MC, Purslow PP. Matrix metalloproteinases are less essential for the in-situ gelatinolytic activity in heart muscle than in skeletal muscle. Comp Biochem Physiol A Mol Integr Physiol 2010;156:518–22. [PubMed: 20427022]

[16]. Huet E, Vallée B, Szul D, Verrecchia F, Mourah S, Jester JV, Hoang-Xuan T, Menashi S, Gabison EE. Extracellular matrix metalloproteinase inducer/CD147 promotes myofibroblast differentiation by inducing alpha-smooth muscle actin expression and collagen gel contraction: implications in tissue remodeling. FASEB J 2008;22:1144–54. [PubMed: 17965264]

[17]. Lijnen P, Petrov V, Fagard R. Transforming growth factor-beta 1-mediated collagen gel contraction by cardiac fibroblasts. J Renin Angiotensin Aldosterone Syst 2003;4:113–8. [PubMed: 12806594]

[18]. Gabbiani G, Ryan GB, Majne G. Presence of modified fibroblasts in granulation tissue and their possible role in wound contraction. Experientia 1971;27:549–50. [PubMed: 5132594]

[19]. Guidry C, Grinnell F. Studies on the mechanism of hydrated collagen gel reorganization by human skin fibroblasts. J Cell Sci 1985;79:67–81. [PubMed: 3914484]

[20]. Margulis A, Nocka KH, Wood NL, Wolf SF, Goldman SJ, Kasaian MT. MMP dependence of fibroblast contraction and collagen production induced by human mast cell activation in a three-dimensional collagen lattice. Am J Physiol Lung Cell Mol Physiol 2009;296:L236–47. [PubMed: 19060229]

[21]. Toriseva MJ, Ala-aho R, Karvinen J, Baker AH, Marjomaki VS, Heino J, Kahari VM. Collagenase-3 (MMP-13) enhances remodeling of three-dimensional collagen and promotes survival of human skin fibroblasts. J Invest Dermatol 2007;127:49–59. [PubMed: 16917496]

[22]. Rohr S Cardiac fibroblasts in cell culture systems: myofibroblasts all along? J Cardiovasc Pharmacol 2011;57:389–99. [PubMed: 21326104]

Author Manuscript Author Manuscript Author Manuscript Author Manuscript

[23]. Santiago J, Dangerfield AL, Rattan SG, Bathe KL, Cunnington RH, Raizman JE, Bedosky KM, Freed DH, Kardami E, Dixon IMC. Cardiac fibroblast to myofibroblast differentiation in vivo and in vitro: expression of focal adhesion components in neonatal and adult rat ventricular myofibroblasts. Dev Dyn 2010;239:1573–84. [PubMed: 20503355]

[24]. Fringer J, Grinnell F. Fibroblast quiescence in floating or released collagen matrices: contribution of the ERK signaling pathway and actin cytoskeletal organization. J Biol Chem 2001;276:31047–52. [PubMed: 11410588]

[25]. Larsen MB, Stephens RW, Brunner N, Nielsen HJ, Engelholm LH, Christensen IJ, Stetler-Stevenson WG, Hoyer-Hansen G. Quantification of tissue inhibitor of metalloproteinases 2 in plasma from healthy donors and cancer patients. Scand J Immunol 2005;61:449–60. [PubMed: 15882437]

[26]. Bildt MM, Bloemen M, Kuijpers-Jagtman AM, Von den Hoff JW. Matrix metalloproteinase inhibitors reduce collagen gel contraction and alpha-smooth muscle actin expression by periodontal ligament cells. J Periodontal Res 2009;44:266–74. [PubMed: 18973523]

[27]. Spinale FG. Myocardial matrix remodeling and the matrix metalloproteinases: influence on cardiac form and function. Physiol Rev 2007;87:1285–342. [PubMed: 17928585]

[28]. Brower GL, Gardner JD, Forman MF, Murray DB, Voloshenyuk T, Levick SP, Janicki JS. The relationship between myocardial extracellular matrix remodeling and ventricular function. Eur J Cardiothorac Surg 2006;30:604–10. [PubMed: 16935520]

[29]. Karsdal MA, Larsen L, Engsig MT, Lou H, Ferreras M, Lochter A, Delaissé J, Foged NT. Matrix metalloproteinase-dependent activation of latent transforming growth factor-beta controls the conversion of osteoblasts into osteocytes by blocking osteoblast apoptosis. J Biol Chem 2002;277:44061–7. [PubMed: 12226090]

[30]. Yu Q, Stamenkovic I. Cell surface-localized matrix metalloproteinase-9 proteolytically activates TGF-β and promotes tumor invasion and angiogenesis. Genes Dev 2000;14:163–76. [PubMed: 10652271]

[31]. Seo DW, Li H, Qu CK, Oh J, Kim YS, Diaz T, Wei B, Han JW, Stetler-Stevenson WG. Shp-1 mediates the antiproliferative activity of tissue inhibitor of metalloproteinase-2 in human microvascular endothelial cells. J Biol Chem 2006;281:3711–21. [PubMed: 16326706]

[32]. Tierney GM, Griffin NR, Stuart RC, Kasem H, Lynch KP, Lury JT, Brown PD, Millar AW, Steele RJ, Parsons SL. A pilot study of the safety and effects of the matrix metalloproteinase inhibitor marimastat in gastric cancer. Eur J Cancer 1999;35:563–8. [PubMed: 10492628]

[33]. Hudson MP, Armstrong PW, Ruzyllo W, Brum J, Cusmano L, Krzeski P, Lyon R, Quinones M, Theroux P, Sydlowski D, Kim HE, Garcia MJ, Jaber WA, Weaver WD. Effects of selective matrix metalloproteinase inhibitor (PG-116800) to prevent ventricular remodeling after myocardial infarction: results of the PREMIER (Prevention of Myocardial Infarction Early Remodeling) trial. J Am Coll Cardiol 2006;48:15–20. [PubMed: 16814643]

[34]. Gibbs CL, Loiselle DS. Cardiac basal metabolism. Jpn J Physiol 2001;51:399–426. [PubMed: 11564278]

Author Manuscript Author Manuscript Author Manuscript Author Manuscript

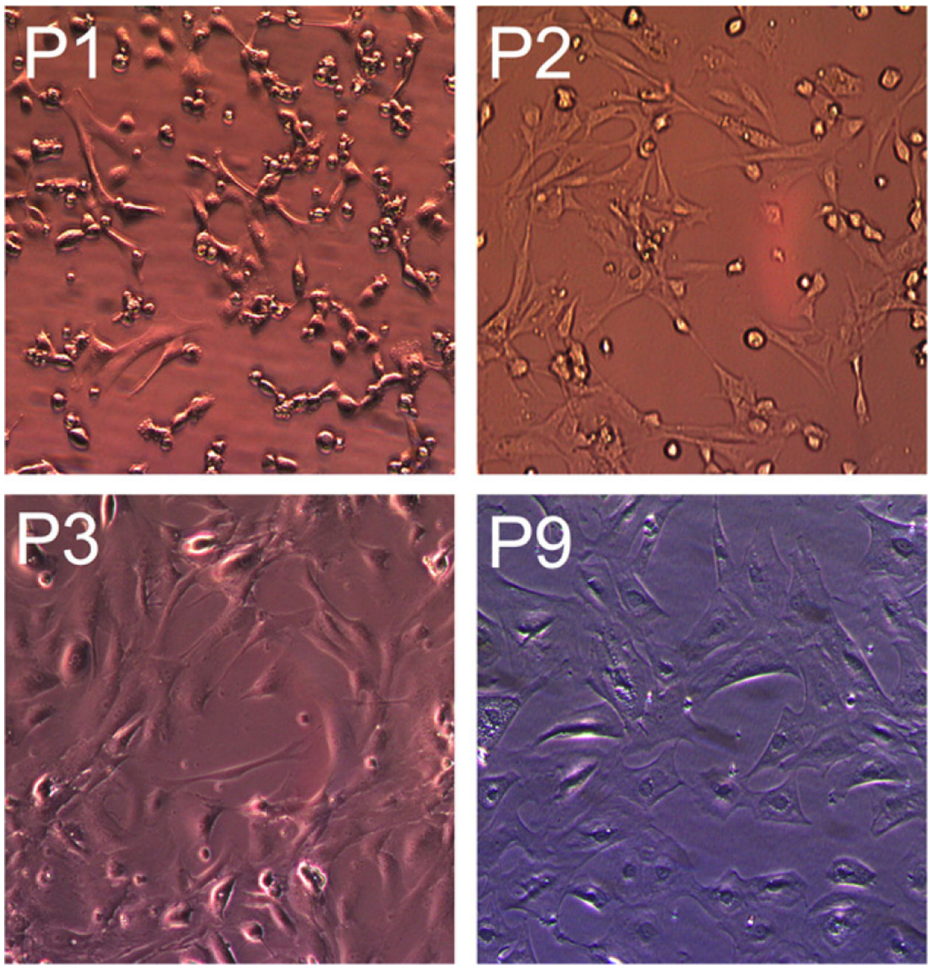

Fig. 1.

Primary human cardiac fibroblasts morphology. Photomicrographs obtained from serial passages of human cardiac fibroblasts from the same isolation. Objective: 20×. Note that the changes in cellular morphology as cell passage increased. Scale bar=100 μm.

Author Manuscript Author Manuscript Author Manuscript Author Manuscript

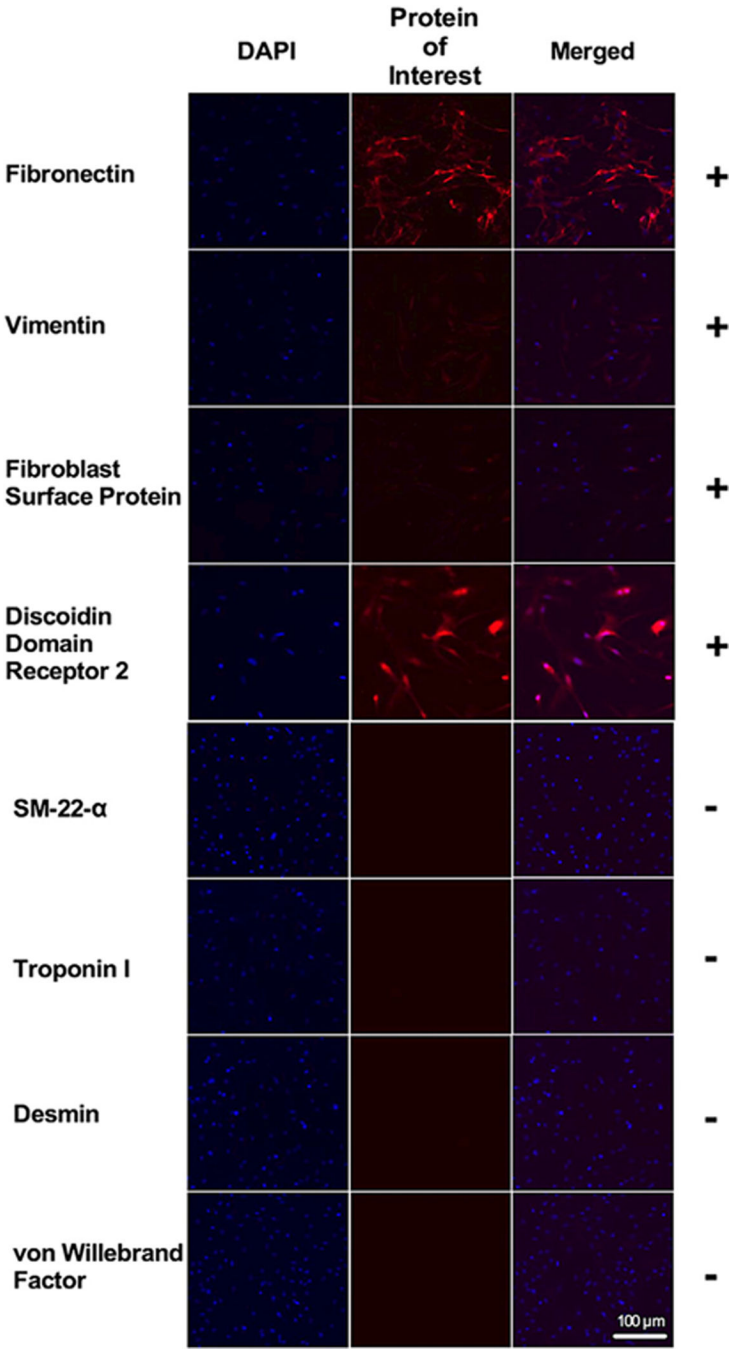

Fig. 2.

Characterization of primary human cardiac fibroblasts. All cultured cells expressed fibronectin, vimentin, FSP, and DDR2, staining with an absence of SM-22-alpha, troponin I, desmin, and vWF staining, confirming these cells as fibroblasts. Nuclei were stained blue with DAPI. FSP=fibroblast surface protein; DDR2=discoidin domain receptor 2; SM-22-a= smooth muscle-22-alpha; vWF=von Willebrand factor.

Author Manuscript Author Manuscript Author Manuscript Author Manuscript

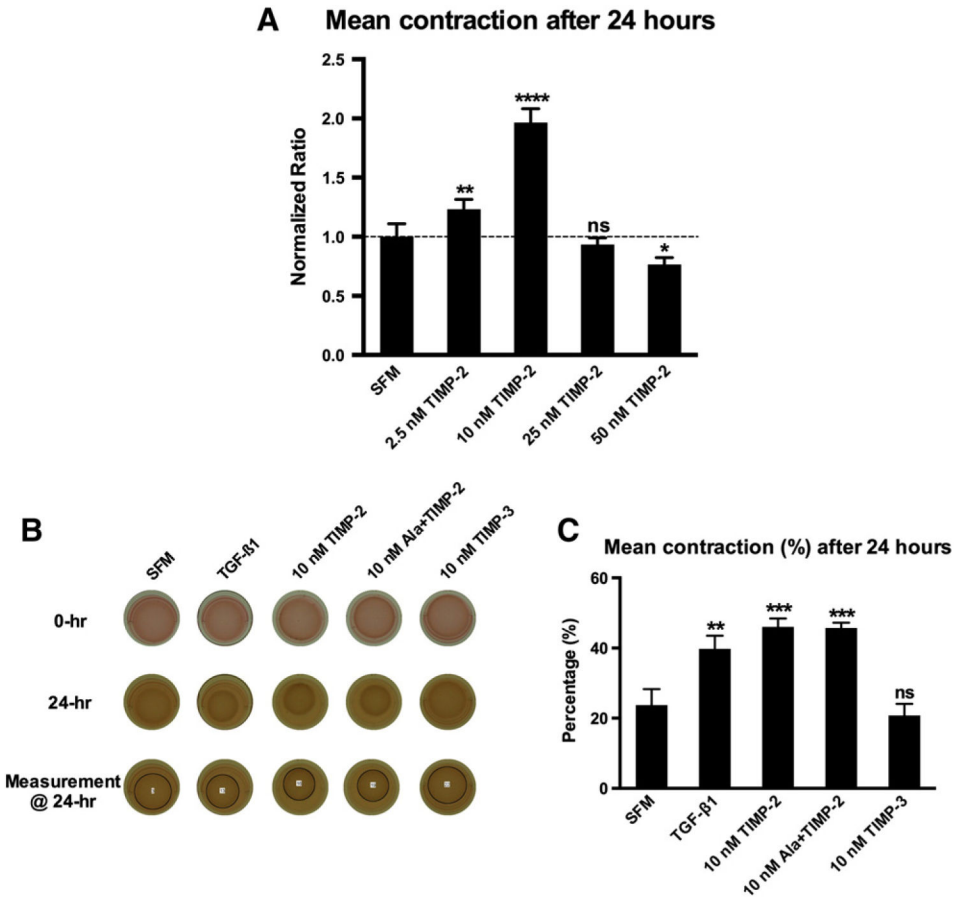

Fig. 3.

Fibroblast-mediated 3D collagen matrix remodeling. (A) Differential effect of various concentrations of TIMP-2 on 3D collagen ECM remodeling as assessed by extent of contraction over time: TIMP-2 stimulated collagen ECM contraction at lower concentrations (2.5 and 10 nM), whereas the highest concentration (50 nM) inhibited ECM contraction when compared to the SFM group. Data presented were obtained from three individual experiments, and all values were normalized to the corresponding SFM control group. Bars represent mean±S.D. (N=7 per group). *P<.05; **P<.01; **** P<.0001. (B) Representative photographs of cell–ECM constructs at 0 and 24 h by treatment group. (C) Percentage of ECM contraction (%) from the initial surface area 24 h after release. TGF-beta1 (10 ng/ml), TIMP-2 and Ala+TIMP-2 significantly stimulated collagen ECM contraction, whereas TIMP-3 did not alter ECM contraction as compared to the SFM group. Bars represent mean ±S.D. (N=3 per group). ** P<.01; *** P<.001; ns, nonsignificant.

Author Manuscript Author Manuscript Author Manuscript Author Manuscript

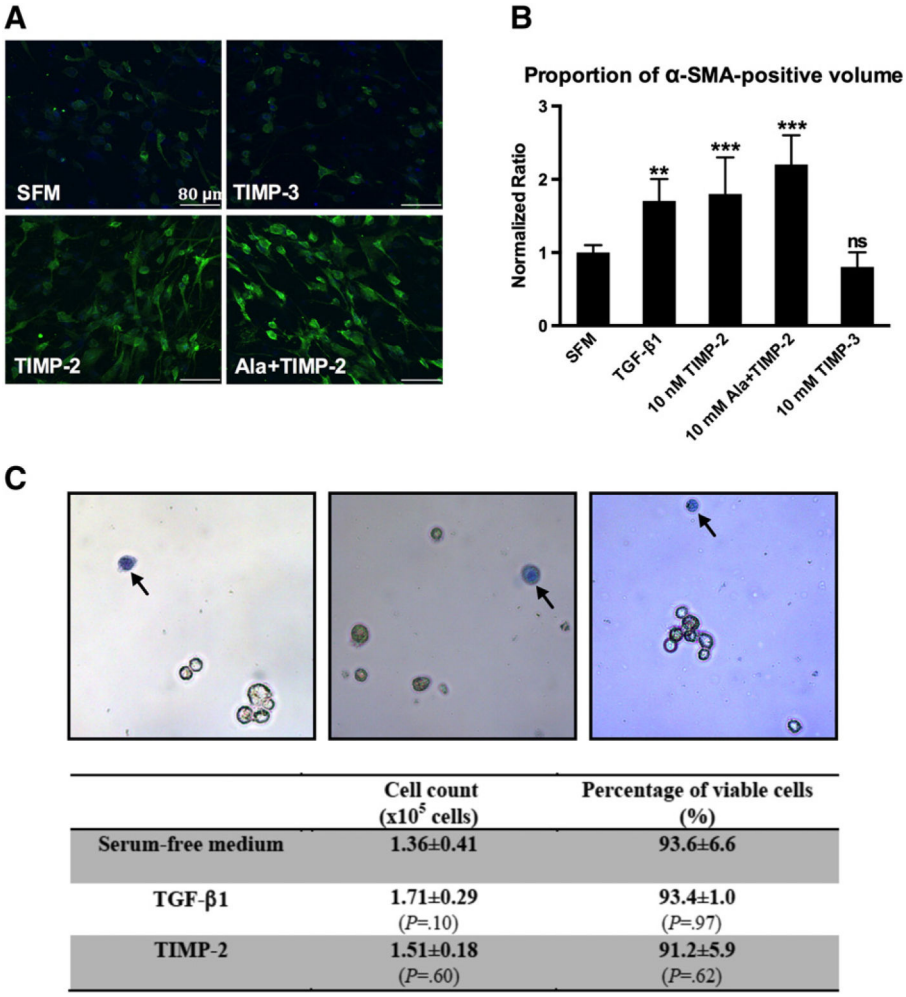

	Cell count ($x10^5$ cells)	Percentage of viable cells (%)
Serum-free medium	1.36±0.41	93.6±6.6
TGF-β1	1.71±0.29 (*P*=.10)	93.4±1.0 (*P*=.97)
TIMP-2	1.51±0.18 (*P*=.60)	91.2±5.9 (*P*=.62)

Fig. 4.

Cardiac myofibroblast activation and cell viability. (A) Representative confocal microscopic images of cardiac fibroblasts/myofibroblasts embedded in collagen ECM constructs from different treatment groups. Cells were stained for alpha-SMA (green) and for nuclei (DAPI, blue). Both TIMP-2 and Ala+TIMP-2 stimulated alpha-SMA expression and induced morphological transformation. TIMP-3 did not exert a similar effect. Scale bar=80 µm. (B) Proportion of confocal image volume stained positive for a-SMA (green). Values were normalized to that of the SFM group. TGF-beta1 (10 ng/ml), TIMP-2 and Ala-TIMP-2 induced a similar increase in expression of alpha-SMA. TIMP-3 did not alter alpha-SMA expression as compared to the SFM group. Bars represent mean±S.D. (*N*=8 random field images per group). ** *P*<.01; *** *P*<.001; ns, nonsignificant. (C) Representative photomicrographs of cells harvested directly from cell–ECM constructs after the exposure to targeted treatments. Dead cells appear blue after trypan blue staining (arrows). Objective: 20×. All treatment groups yielded an equal cell number and cell viability (*N*=8 per group).

Author Manuscript Author Manuscript Author Manuscript Author Manuscript

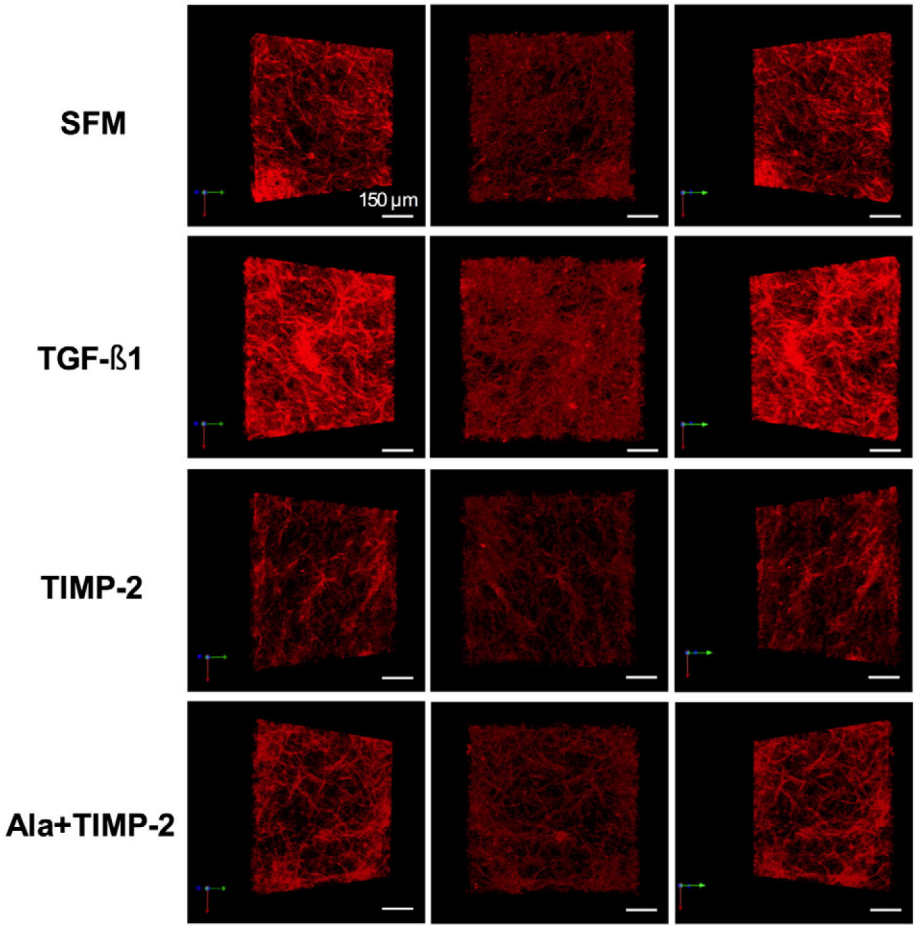

Fig. 5.

3D collagen matrix architecture. 3D images of collagen ECM architecture were reconstructed. Each row consists of three different projections of one representative image of a cell–ECM construct for each treatment group. Scale bar=150 µm. *Top row*: SFM group, which represents the baseline state with an assumption that ECM homeostasis is maintained (negative control). *Second row*: TGF-beta1 increased collagen fibril density in the cell–ECM construct showing a net accumulation of collagen (fibrosis) relative to the SFM control. *Third row*: TIMP-2 did not increase the density of collagen, instead a modest amount of ECM degradation was observed as compared to SFM. Bottom row: Ala+TIMP-2 did not significantly alter the collagen ECM architecture as compared to SFM.

Author Manuscript Author Manuscript Author Manuscript Author Manuscript

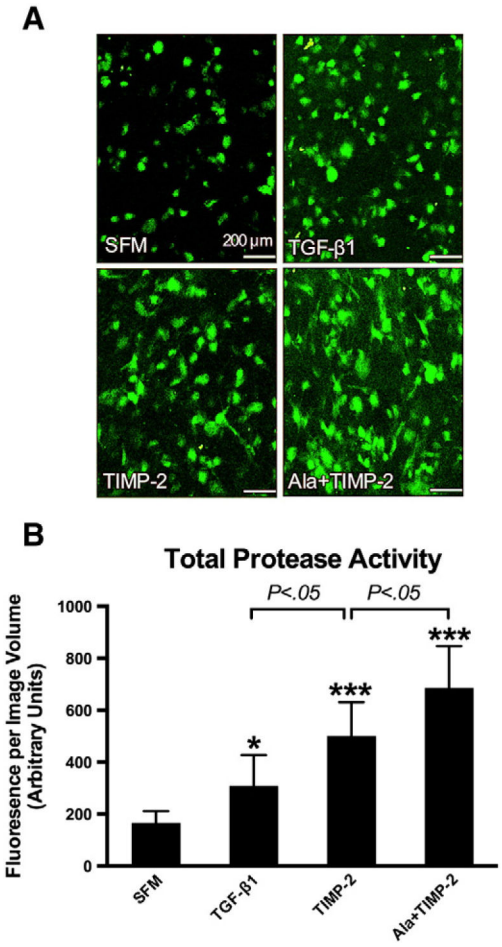

Fig. 6.

In situ zymography with quantitative assessments of total protease activity in collagen ECM microenvironment. (A) In situ zymography: representative confocal microscopic images of the emitted fluorescent signals (green) in collagen ECM, following proteolysis of the embedded DQ Gelatin-FITC. Scale bar=200 μm. (B) Total protease activity in cell–ECM constructs was quantified as total fluorescent signal per image volume. TGF-beta1 (10 ng/ml), TIMP-2 (10 nM) and Ala+TIMP-2 (10 nM) increased the total protease activity in the ECM microenvironment as compared to SFM. TIMP-2 yielded more protease activity than TGF-beta1 ($P<.05$). Ala+TIMP-2 resulted in a higher protease activity than TIMP-2, likely due to a lack of MMP inhibition ($P<.05$). Bars represent mean±S.D. ($N=8$ per group). * $P<.05$; *** $P<.001$ as compared to SFM.

Author Manuscript Author Manuscript Author Manuscript Author Manuscript

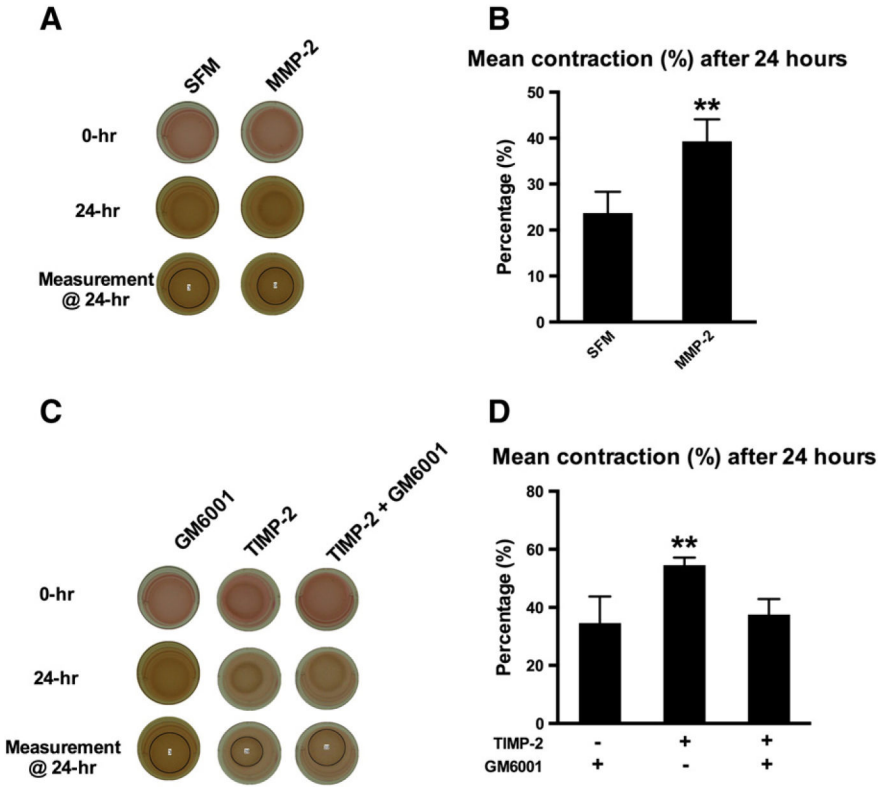

Fig. 7.

Effects of MMP-2 and MMP inhibition on cardiac myofibroblast differentiation. (A) Representative photographs of cell–ECM constructs at 0 and 24 h: collagen ECM remodeling was differentially assessed with or without addition of activated MMP-2 (100 ng/ml). (B) Activated MMP-2 induced cardiac myofibroblast-mediated collagen ECM remodeling. Bars represent mean±S.D. (N=3 per group). ** P<.01. (C) Representative photographs of cell–ECM constructs at 0 and 24 h: the effect of TIMP-2 on collagen ECM remodeling was evaluated alone and in the presence of GM6001 (MMP inhibitor). (D) TIMP-2 stimulated collagen ECM remodeling. Addition of GM6001 inhibited TIMP-2-induced ECM remodeling. These data suggest that TIMP-2 stimulates cardiac myofibroblast differentiation by increasing protease activity. Bars represent mean±S.D. (N=3 per group). * P<.05; ** P<.01.